Parametric Study and Temperature Sensitivity of Microstrip Antennas Using an Improved Linear Transmission Line Model

Sarath Babu and Girish Kumar, *Senior Member, IEEE*

***Abstract*—An improved linear transmission line (LTL) model has been developed after incorporating several modifications in the reported linear transmission line model for analyzing arbitrarily shaped microstrip antennas (MSA's), which should be symmetrical with respect to the feed axis. Simulations have been carried out for rectangular, circular, and equilateral triangular MSA's and the results are in good agreement with reported results. A parametric study for these MSA's has also been performed. A study of the temperature sensitivity for rectangular MSA's for different types of substrates has been carried out. An MSA utilizing a substrate with a lower dielectric constant and thermal coefficient is less sensitive to temperature variations.**

***Index Terms*—Printed antennas, thermal factors.**

I. Introduction

A linear transmission line (LTL) model was previously reported [1], [2] to model a microstrip antenna (MSA) of arbitrary shape and constant thickness which is symmetrical with respect to the z axis as shown in Fig. 1. For a rectangular MSA, the dominant mode of propagation is a TEM or quasi-TEM mode having negligible variation of fields in the transverse direction. The same concept is applied to the MSA of arbitrary shape provided it is linearly polarized along the symmetrical axis. The characteristic conductance $G_c(z)$ and the propagation coefficient per unit length $\gamma(z)$ due to the radiation, dielectric, and metallic losses are not constant along such a transmission line. Hence, an appropriate width $W(z)$ (perpendicular to the axis of symmetry) is selected. In this method, the patch is divided into very small sections along the feed axis and then the width for each section is calculated.

II. Formulation of the LTL Model

The normalized radiation admittance Y_r with respect to $G_0 = 1/(120\pi)$ is given by [1], [2]

$$\frac{dY_r(y)}{dy} + \left[\frac{4\pi^3 {H_r}^2}{5\sqrt{\epsilon_e}} g_c(y) + \pi\sqrt{\epsilon_e}\left(\tan\delta + \frac{D_s}{H_r}\right) + j2\pi\sqrt{\epsilon_e}\right] * \left[g_c(y) - \frac{{Y_r}^2(y)}{g_c(y)}\right] = 0. \quad (1)$$

With $y = z/\lambda_o$, $g_c(y) = G_c(y)/G_0$, $Y_r = Y(y)/G_0$, $H_r = h/\lambda_o$, and $D_s = \sqrt{\epsilon_o f/\pi\sigma}$. The $G_c(z)$ and ϵ_e are the characteristic admittance and effective dielectric constant corresponding to the width $W(z)$ of the patch at z.

Manuscript received March 6, 1997; revised June 12, 1998.

The authors are with the Electrical Engineering Department, I.I.T. Powai, Mumbai, 400076 India.

Publisher Item Identifier S 0018-926X(99)03727-8.

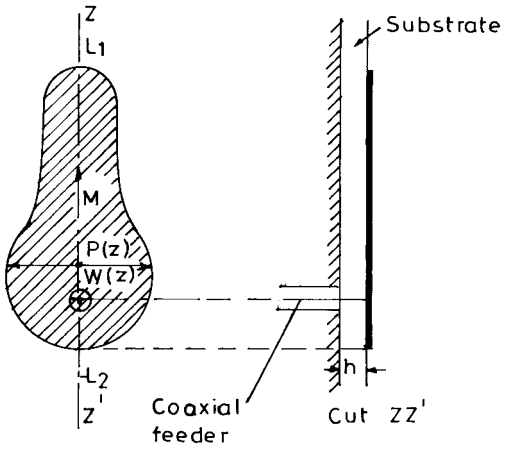

Fig. 1. Arbitrary-shaped patch antenna with coaxial feed.

For the coaxial feed point located along the symmetrical axis (shown in Fig. 1), the limiting conditions are: $Y_{r1}(L_1/\lambda_o) = 0$ and $Y_{r2}(-L_2/\lambda_o) = 0$.

III. Improved LTL Model

The above reported model does not include the effects of fringing fields and the dispersion effect and, therefore, the resonant frequency and input impedance calculated were not in good agreement with the measured results. The following modifications are proposed to improve the previously reported LTL model.

- The effective dimensions of the antennas are used instead of the physical dimensions to account for the fringing fields.
- The effective permittivity and the characteristic admittance equations are used to account for the dispersion effect [3].
- The effect of probe inductance is taken into account [4]

$$X_L = \frac{120}{\sqrt{\epsilon_r}} \tan\frac{\pi\sqrt{\epsilon_r}h}{\lambda_o} \ln\frac{2.25\lambda_o}{2\pi\sqrt{\epsilon_r}d} \quad (2)$$

where d is the diameter of the probe.

After incorporating the above modifications, the improved LTL model has been used to analyze several rectangular microstrip antennas (RMSA), circular microstrip antennas

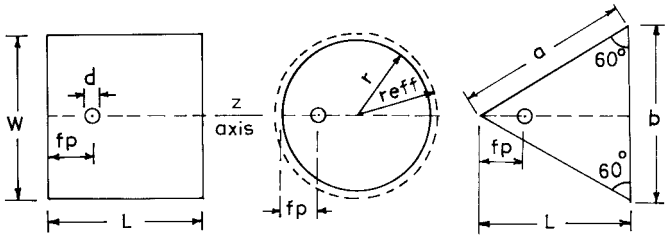

Fig. 2. Rectangular, circular, and equilateral triangular MSA.

TABLE I
COMPARISON OF RESULTS FOR RMSA

Case No	ϵ_r	h	L	W	fp	Reported		Simulated	
						fr	Rr	fr	Rr
		cm	cm	cm	cm	MHz	ohms	MHz	ohms
1	10.2	0.127	2.00	3.00	0.650	2260	85	2281	100
2	10.2	0.127	0.95	1.50	0.320	4490	53	4589	89
3	10.2	0.254	1.90	3.00	0.650	2240	80	2296	83
4	2.22	0.079	2.50	4.00	0.400	3940	89	3906	75
5	2.22	0.079	1.25	2.00	0.200	7650	99	7572	76
6	2.22	0.152	2.50	4.00	0.400	3840	87	3802	74
7a	2.62	0.159	7.62	11.43	2.290	1192	47	1197	42
7b	2.62	0.159	7.62	11.43	0.760	1190	125	1196	111
8a	2.50	0.159	4.14	6.858	1.016	2222	51	2218	51
8b	2.50	0.159	4.14	6.858	0.100	2215	111	2213	107

(CMSA), and equilateral triangular microstrip antennas (ETMSA).

IV. SIMULATION OF RMSA

In case of the RMSA, shown in Fig. 2, the width function $W(z)$ is equal to the width W of the rectangular patch. The effective length of the patch accounting for the fringing fields effect is given by $L_{\text{eff}} = L + 2\Delta l$. The Δl is the extension in length computed from expressions in [3].

Simulations have been carried out for the RMSA using the modified LTL model and the results are compared with the reported experimental results [5]–[7]. The dimensions of the RMSA and the measured resonant frequency and resonant resistance along with the simulated values are shown in Table I. The error in the simulated resonant frequency is less than 1% for all the cases except for the thicker substrates with a high dielectric constant for which it is around 2%. The input impedance computed is in agreement with the measured impedance values. The simulated and reported impedance loci for cases 7 and 8 are shown in Figs. 3 and 4. The f_1 and f_2 shown in the impedance plot indicate the lower and upper frequency limits and Δf indicates the increment in frequency.

V. PARAMETRIC STUDY OF RMSA

The effects of varying various parameters of a RMSA such as, length, width, dielectric constant, substrate thickness, and loss tangent (tan δ) have been carried out using the LTL model.

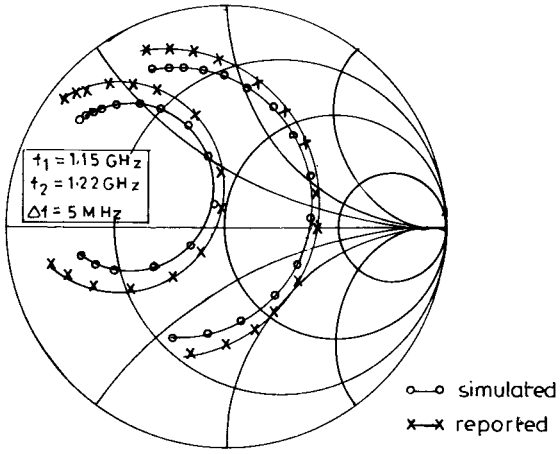

Fig. 3. Impedance plot of RMSA for case 7.

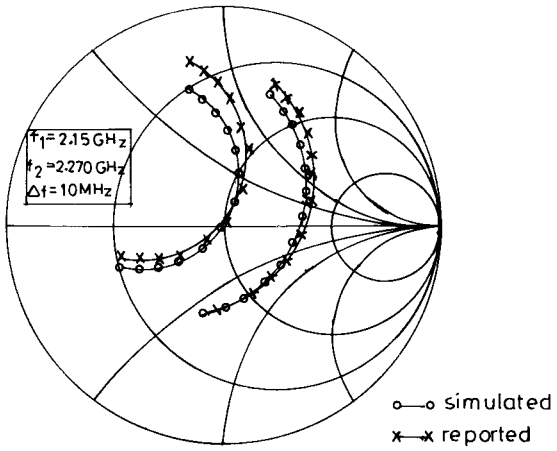

Fig. 4. Impedance plot of RMSA for case 8.

The variations could be either due to manufacturing tolerances or due to temperature change.

The dimensions of the RMSA have been taken as: $W = 4$ cm; $L = 3$ cm; $h = 0.16$ cm; $\epsilon_r = 2.55$; and $\tan \delta = 0.001$.

The input impedance, resonant frequency and bandwidth (BW) for variations in different parameters are tabulated in Table II for a feedpoint location 2.15 cm from the edge. As expected, the resonant frequency varies inversely with the antenna dimensions. The change is more pronounced with the variation in L as compared to a variation in W. Also, BW decreases with an increase in L. The input impedance loci for three different lengths and widths are shown in Figs. 5 and 6. With an increase in W, the input impedance loci on the Smith chart shifts upward and toward the left and with an increase in L, it shifts downward and toward the left. The plots are for the normalized feed point with a variation in length.

The resonant frequency and bandwidth vary inversely with respect to the dielectric constant also. The input impedance loci for different ϵ_r are plotted in Fig. 7. The impedance loci shifts downward and toward the left with an increase in ϵ_r.

In the case of small changes in h, there is no significant variation in the resonant frequency. If h is increased significantly, then the resonant frequency decreases due to an increase in open-end fringing fields and the bandwidth increases. The

TABLE II
RESULTS OF SENSITIVITY STUDY FOR RMSA

Design values: W = 4 cm, L = 3 cm, h = 0.16 cm, $\epsilon_r = 2.55$, $\tan\delta = 0.001$

Parameters Varied	fp (cm)	Frequency (GHz)	Input Impedance	VSWR	BW * (MHz)
Design values	2.15	3.002	57.18–j0.14	1.14	88
W = 4.2 cm	2.15	3.002	51.60–j0.21	1.03	90
W = 4.5 cm	2.15	3.003	44.30+j0.07	1.13	88
L = 3.15 cm	2.258	2.866	63.26–j0.35	1.27	78
L = 3.3 cm	2.365	2.741	69.84+j0.61	1.40	69
L = 3.15 cm W = 4.2 cm	2.258	2.865	57.57–j0.23	1.15	81
L = 3.15 cm W = 4.2 cm h = 0.168 cm	2.258	2.859	57.38+j0.32	1.15	84
$\epsilon_r = 2.32$	2.15	3.142	51.27+j0.19	1.03	101
$\epsilon_r = 2.80$	2.15	2.870	63.51+j0.20	1.27	76
h = 0.08 cm	2.15	3.067	59.03+j0.28	1.18	50
h = 0.24 cm	2.15 cm	2.956	46.11–j0.06	1.08	117
$\tan\delta = 0.005$	2.15	3.007	50.17–j0.38	1.01	94
$\tan\delta = 0.01$	2.15	3.013	43.48+j0.52	1.15	99

* BW is for VSWR 2.

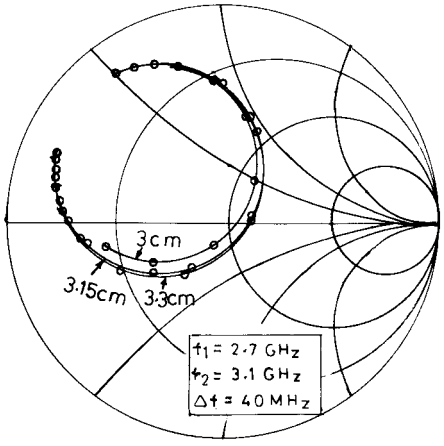

Fig. 5. Impedance loci of RMSA for three lengths.

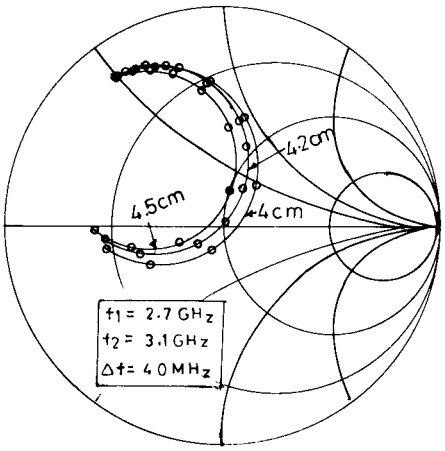

Fig. 6. Impedance loci of RMSA for three widths.

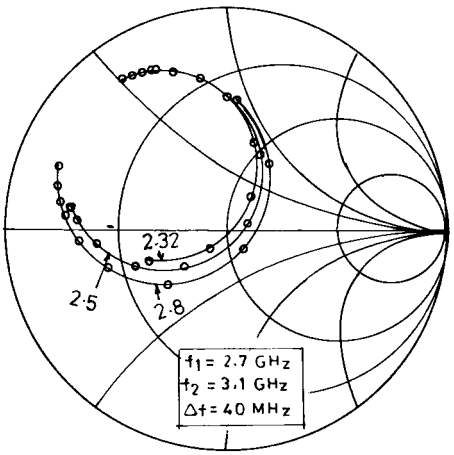

Fig. 7. Impedance loci of RMSA for three dielectric constants.

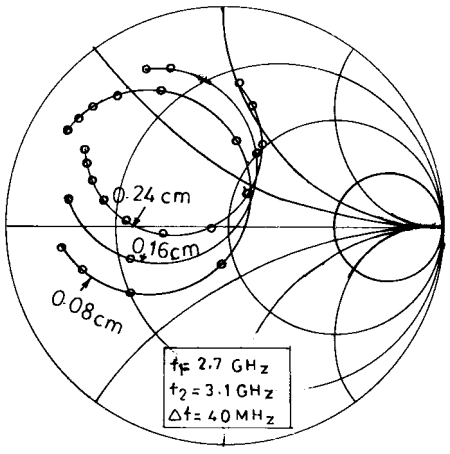

Fig. 8. Impedance loci of RMSA for three substrate thicknesses.

input impedance loci for different values of h are plotted in Fig. 8. The plot shifts upward and toward the right due to the large inductive probe reactance.

The input impedance loci for three different values of tan δ are plotted in Fig. 9. With an increase in the value of tan δ, the impedance plot shifts toward the left side of the Smith chart due to an increase in the losses in the dielectric substrate. However, the change in the resonant frequency is very small.

VI. TEMPERATURE SENSITIVITY OF RMSA

The resonant frequency of a MSA is sensitive to large temperature variations. There are two major factors affecting the resonant frequency of a microstrip radiator exposed to large temperature variations [8].

A. Metallic Expansion or Contraction

The metallic expansion or contraction of the radiating patch due to a change in temperature affects the resonant frequency. With an increase in temperature, the metallic patch expands,

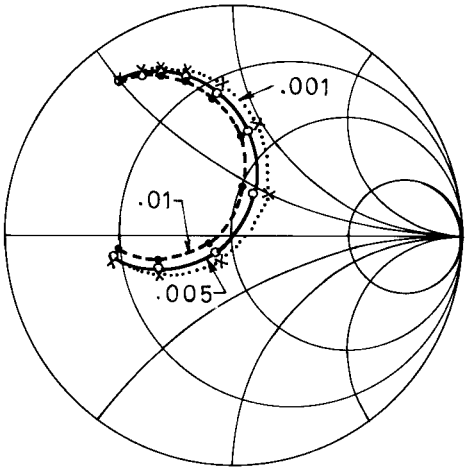

Fig. 9. Impedance loci of RMSA for three values of $\tan\delta$.

making the effective resonant dimension longer and, therefore, decreasing the operating frequency. The relative frequency change for dimensional changes may be expressed in terms of linear dimensions or in terms of temperature changes as follows [9]:

$$\frac{\delta f}{f_o} = -\frac{\delta L}{L} = -\alpha_d \delta T \tag{3}$$

where

δf change in resonant frequency;
δL change in effective resonant dimension;
α_d thermal coefficient of expansion;
δT temperature change in °C.

B. Effective Dielectric Constant Change

Most of the substrates which are generally used for microwave applications like polytetra fluroethylene (PTFE)-based materials, Teflon/Fiberglass reinforced materials, and ceramic powder filled TFE (epsilam) materials exhibit a decrease in dielectric constant with an increase in temperature. The change in operating frequency of a MSA due to a small change in ϵ_r can be expressed as follows [9]:

$$\frac{\delta f}{f_o} = -\frac{1}{2}\frac{\delta \epsilon_r}{\epsilon_r} = +\frac{1}{2}\alpha_\epsilon \delta T \tag{4}$$

where

$\delta\epsilon_r$ change in ϵ_r;
α_ϵ thermal coefficient of dielectric constant.

Combining (3) and (4), the change in resonant frequency due to a temperature variation δT is given by

$$\frac{\delta f}{f_o} = \left(-\alpha_d + \frac{1}{2}\alpha_\epsilon\right)\delta T. \tag{5}$$

C. Results of the Temperature Sensitivity Study

The temperature sensitivity study of a RMSA has been carried out for three different commercially available substrates. The dimensions of the RMSA for all three cases have been taken same as: $W = 4$ cm; $L = 3$ cm; and $h = 0.159$ cm. The thermal coefficient of expansion of copper is $17 \times 10^{-6}/°\text{C}$.

TABLE III
RESULTS OF TEMPERATURE SENSITIVITY STUDY

Substrate	Temp. °C	Variations in	Frequency GHz	VSWR	BW MHz
RT DUROID 5500	+25		3.033	1.07	92
	-40	dimensions	3.036	1.06	92
		ϵ_r	3.022	1.08	91
		both	3.025	1.08	92
	+60	dimensions	3.031	1.07	92
		ϵ_r	3.039	1.06	93
		both	3.037	1.06	93
RT DUROID 6006	+25		1.991	1.02	20
	-40	dimensions	1.993	1.02	20
		ϵ_r	1.968	1.01	20
		both	1.970	1.02	20
	+60	dimensions	1.990	1.02	22
		ϵ_r	2.003	1.02	20
		both	2.002	1.02	20
EPSILAM 10	+25		1.529	1.02	9
	-40	dimensions	1.530	1.02	8
		ϵ_r	1.501	1.05	8
		both	1.503	1.03	8
	+60	dimensions	1.528	1.02	9
		ϵ_r	1.544	1.01	9
		both	1.543	1.03	9

In case 1, a RT/Duroid 5500 substrate is considered with the following specifications: $\epsilon_r = 2.5$; $\tan\delta = 0.0025$; and $\alpha_\epsilon = -110$ ppm/°C. For an input impedance equal to 50 Ω, the proper feedpoint is found to be 2.15 cm from the edge. A comparative study of the resonant frequency at −40 °C and +60 °C is carried out with respect to the resonant frequency at room temperature. The effective parameters of the RMSA at −40 °C are $W = 3.9956$ cm, $L = 2.9967$ cm, and $\epsilon_r = 2.518$. To compensate for the change in L, the feedpoint is placed 2.1476 cm from the edge. The effective parameters at +60 °C are $W = 4.0024$ cm, $L = 3.0017$ cm, and $\epsilon_r = 2.490$. The feed point is now located 2.1513 cm from the edge. The change in substrate thickness due to temperature variation is not considered since it is negligible. The simulated results are tabulated in Table III.

In case 2, a RT DUROID 6600 substrate is considered with the following specifications: $\epsilon_r = 6.0$, $\tan\delta = 0.0025$, and $\alpha_\epsilon = 370$ ppm/°C. The feedpoint is taken at 1.92 cm from the edge at room temperature. The calculated dielectric constant at −40 °C is 6.1443 and at +60 °C it is 5.9223. The feedpoint is taken at 1.9179 cm for −40 °C and at 1.9211 cm for +60 °C. The simulated results are given in Table III.

In case 3, an Epsilam-10 substrate is considered with the following parameters: $\epsilon_r = 10.3$, $\tan\delta = 0.002$, and $\alpha_\epsilon = 570$ ppm/°C. The feedpoint is taken at 1.855 cm from the edge. The calculated dielectric constant at −40 °C is 10.682; and at

TABLE IV
COMPARISON OF RESULTS FOR CMSA

Case No	ϵ_r	r cm	h cm	fp cm	Reported fr(MHz)	Simulated fr(MHz)	%error
1	2.50	3.493	0.1588	2.43	1570	1546	-1.53
2	2.59	1.270	0.0794	1.65	4070	4110	+0.98
3	2.50	3.493	0.3175	2.30	1510	1535	+1.65
4	2.70	13.894	1.2700	9.00	378	374	-1.06
5	4.55	4.950	0.2350	3.75	825	815	-1.21
6	4.55	3.975	0.2350	3.03	1030	1006	-2.33
7	4.55	2.990	0.2350	2.25	1360	1367	+0.51
8	4.55	2.000	0.2350	1.48	2003	2012	+0.45
9	4.55	1.040	0.2350	0.73	3750	3715	-0.93
10	4.55	0.770	0.2350	0.51	4945	4884	-1.23
11a	2.62	6.700	0.1590	5.02	798	805	+0.88
11b	2.62	6.700	0.1590	1.67	795	805	+1.25
12	2.20	3.000	0.1590	2.05	1920	1898	-1.15
13	2.50	4.190	0.1590	3.17	1304	1298	-0.46

+60 °C it is 10.095. The feedpoint is taken at 1.8529 cm for −40 °C and at 1.8561 cm for +60 °C. The simulated results are tabulated in Table III.

From Table III, it is noted that the resonant frequency varies directly with temperature. This variation is negligible if the dielectric constant is small. But as the dielectric constant increases, the variation due to temperature changes becomes significant. Also, this effect is greater when α_ϵ is large.

VII. SIMULATION OF CMSA

For a CMSA shown in Fig. 2, the width function $W(z)$ is given by

$$W(z) = 2r \sin\left\{2 \arccos\sqrt{\frac{z}{2r}}\right\}. \tag{6}$$

The effective radius r_{eff} has been calculated using the following expression [10]:

$$r_{\text{eff}} = r\left\{1 + \frac{2h}{\pi r \epsilon_r} \cdot \left[\ln\frac{r}{2h} + 1.41\epsilon_r + 1.77 + \frac{h}{r}(0.268\epsilon_r + 1.65)\right]\right\}^{1/2}. \tag{7}$$

In the analysis, ϵ_r is used for smaller h/r and ϵ_{dyn} [11] is used for larger h/r since the capacitive effect of a CMSA increases with h/r. Simulations have been carried out for different radii and substrate parameters for the CMSA. The reported [6], [7], [11] and simulated results are tabulated in Table IV. The feed point locations are specified only for the last four cases in the reported results and, hence, the feed point locations are calculated for the other cases to match a 50 Ω input impedance. The error in the resonant frequency for most of the cases is around 1%; however, the error in the worst case is 2.33%. The simulated and reported input impedance loci for case 12 are shown in Fig. 10. The simulated impedance loci is in close agreement with the one reported.

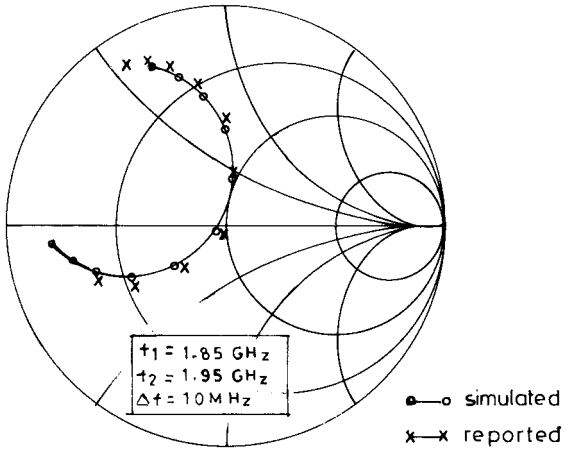

Fig. 10. Impedance plot of CMSA.

TABLE V
COMPARISON OF RESULTS FOR ETMSA

ϵ_r	a cm	h cm	fp cm	Measured fr(MHz)	Moment fr(MHz)	LTL Method fr(MHz)	%error
2.32	8.7	0.078	0.50	1489	1498	1522	+1.60
2.32	8.7	0.078	5.49	-	1498	1523	+1.67
2.32	10.0	0.050	6.34	-	1299	1348	+3.77
2.32	10.0	0.100	6.31	-	1294	1319	+1.93
2.32	10.0	0.159	0.30	1280	1288	1290	+0.16
2.32	10.0	0.159	6.31	-	1288	1291	+0.23
2.32	10.0	0.200	6.32	-	1284	1274	-0.78
10.00	10.0	0.400	5.80	-	639	634	-0.78
10.50	4.1	0.070	0.50	1519	1522	1507	-0.98
10.50	4.1	0.070	2.36	-	1522	1507	-0.98

VIII. SIMULATION OF ETMSA

For the ETMSA shown in Fig. 2, the width function is given by

$$W(z) = z * b/L. \tag{8}$$

The effective dimensions of the ETMSA have been obtained by equating its area to an equivalent CMSA [12]. The r_{eff} of this equivalent circle is calculated and the effective dimension of the ETMSA is calculated from this extended circle. As in the case of the CMSA, ϵ_{dyn} is used in the analysis for larger h/a. The simulated results along with the dimensions and reported results [13] are tabulated in Table V. The feed point of only three cases are given in the reported results; and hence, feed points are selected to match a 50-Ω input impedance for all the other cases. The error indicated is with respect to the simulated results using the moment method. The error is less than 2% for most of the cases.

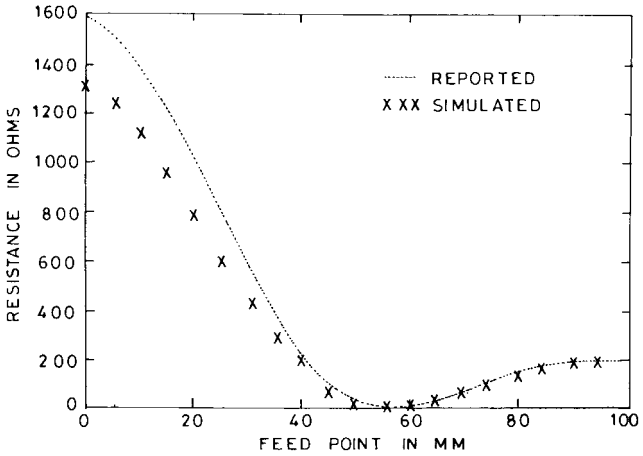

Fig. 11. Resonance resistance of ETMSA versus feedpoint.

The resonance resistance at various feed points as we move from the tip of the triangle to the base was computed for the fundamental mode of an ETMSA with side $s = 10$ cm, $\epsilon_r = 2.32$, and $h = 0.159$ cm. The simulated input resistance variation along the feedpoint axis is in good agreement with the reported variation [14] as shown in Fig. 11.

The parametric studies of the CMSA and the ETMSA have been also carried out with similar results as that of the RMSA.

IX. Conclusion

The analysis of rectangular, circular, and equilateral MSAs has been carried out using an improved linear transmission line model. The simulated resonant frequency and input impedance values are in good agreement with the reported experimental and theoretical values. For most of the cases, the error in resonant frequency is within 2%.

The advantages of the improved LTL model are its faster speed of computation and reasonably good accuracy. However, the disadvantages are that the antenna should be symmetrical with respect to the feed axis and the variation along the width should be small. Therefore, the simulation should not be used for predicting higher order modes and circular or orthogonal polarization of a MSA.

Using the improved transmission line model, the effects of varying the patch dimensions and substrate parameters on the input impedance and resonant frequency have been investigated. Also, a study of the temperature sensitivity of RMSA's has been carried out for three different substrates. It has been observed that the MSA's fabricated on the substrates having a low dielectric constant and a small thermal coefficient are least affected by temperature.

References

[1] G. Dubost, "Linear transmission line model analysis of arbitrary shaped patch antennas," *Electron. Lett.*, vol. 22, no. 15, pp. 798–799, July 1986.
[2] G. Dubost, "Linear transmission line model analysis of a circular patch antenna," *Electron. Lett.*, vol. 22, no. 22, pp. 1174–1176, Oct. 1986.
[3] R. K. Hoffman, *Handbook of Microwave Integrated Circuits.* Norwood, MA: Artech House, 1987.
[4] J. S. Dahele, P. S. Hall, and P. M. Haskins,, *6th Int. Conf. Antennas Propagat.*, Coventry, U.K., Apr. 1989.
[5] D. H. Schaubert, D. M. Pozar, and A. Adrian, "Effect of microstrip antennas substrate thickness and permittivity: Comparison of theories with experiment," *IEEE Trans. Antennas Propogat.*, vol. 37, pp. 677–682, June 1989.
[6] W. F. RichardsY. T. Lo, and D. D. Harrison, "An improved theory for microstrip antennas and applications," *IEEE Trans. Antennas Propagat.*, vol. AP-29, pp. 38–46, Jan. 1981.
[7] Y. Suzuki and T. Chiba, "Computer analysis method for arbitrary shaped microstrip antenna with multi terminals," *IEEE Trans. Antennas Propagat.*, vol. AP-32, pp. 585–590, June 1984.
[8] M. A. Weiss, "Temperature compensation of microstrip antennas," in *IEEE Antennas Propagat. Soc. Int. Symp. Dig.*, Losa Angeles, CA, June 1981, vol. 1, pp. 337–349.
[9] K. R. Carver and J. W. Mink, "Microstrip antenna technology," *IEEE Trans. Antenna Propagat.*, vol. AP-29, pp. 2–24, Jan. 1981.
[10] W. C. Chew and J. A. Kong, "Effects of fringing fields on the capacitance of circular microstrip disk," *IEEE Trans. Microwave Theory Tech.*, vol. MTT-28, pp. 98–104, Feb. 1980.
[11] N. Kumprasert and W. Kiranon, "Simple and accurate formula for the resonant frequency of circular microstrip disk antenna," *IEEE Trans. Antennas Propagat.*, vol. 43, pp. 1331–1333, Nov. 1995.
[12] R. Garg and S. A. Long, "An improved formula for the resonant frequencies of the triangular microstrip patch antennas," *IEEE Trans. Antennas Propagat.*, vol. 36, p. 570, Apr. 1988.
[13] Wei Chen, K. F. Lee, and J. S. Dahele, "Theoretical and experimental studies of the resonant frequencies of the equilateral triangular microstrip antenna," *IEEE Trans. Antennas Propagat.*, vol. 40, pp. 1253–1256, Oct. 1992.
[14] J. R. James, P. S. Hall, and C. Wood, *Microstrip Antenna Theory and Design.* London, U.K.: Peter Peregrinus, 1981.

Sarath Babu was born in Nangiar Kulangara, Kerala, India, on July 14, 1961. He received the B.E. degree in electronics from the Bangalore University, Bangalore, India, in 1983, and the M.Tech. degree in electrical engineering from the Indian Institute of Technology, Bombay, India, in 1997.

He is a Commissioned Officer in the Indian Air Force. His interests are in the areas of microstrip antennas, communication, and radar.

Mr. Babu was elected as an Associate Member of the Institute of Electronics and Telecommunication Engineers in 1989.

Girish Kumar (S'80–M'84–SM'91) was born in Patna, Bihar, India, in June 1957. He received the B.Sc. (electrical engineering) degree from the Aligarh Muslim University, Aligarh, India, in 1978, and the Ph.D. degree (electrical engineering) from the Indian Institute of Technology, Kanpur, India, in 1983.

From 1983 to 1985, he was a Research Associate in the Department of Electrical Engineering, University of Manitoba, Winnipeg, Canada. From 1985 to 1991 he was an Assistant Professor in the Department of Electrical Engineering, University of North Dakota, Grand Forks. Since 1991 he has been an Associate Professor in the Department of Electrical Engineering, Indian Institute of Technology, Bombay, India. His current research interests are in the areas of microstrip antennas, broad-band antennas, and microwave integrated circuits. He has authored or coauthored more than 50 papers and publications.